Experimental Material Characterization and Formability studies on Aluminium Alloy (AA 8011)

Kuraku Ratna Babu[1], *sattenapelli* prashanth[1*], *Kethe* Ganesh[1], *Gone* kiran kumar[1]

[1]Department Of Mechanical Engineering, Gokaraju Rangaraju Institute of Engineering and Technology, Hyderabad, Telangana, India.

Abstract: Operations for sheet metal shaping are essential to the production of many different kinds of goods. But there is still a problem with plastic fragility in this industry, which frequently results in faulty goods. To solve this problem during production, it's critical to take into account a number of factors, including the Forming Limit Diagram (FLD). In this work, the formability of the Aluminum Alloy (AA8011) at strain rates of 0.01 mm/s at ambient temperature, 100 °C, and 150 °C has been investigated. The Nakajima test was used to execute stretch forming in order to achieve the study's results. The material's restricting stresses increased as temperatures increased, according to the outcomes, which were examined utilizing fractography investigations carried out under a scanning electron microscope and simulations carried out with LS-dyna software. This work will help create more productive and successful sheet metal-forming techniques by offering insightful information on the formability of AA 8011 sheet at extreme temperatures.

1 Introduction

The distinctive properties of aluminum alloys, such as their small weight, outstanding thermal conductivity, and exceptional formability, make them useful in a variety of sectors. Because of these qualities, aluminum alloys may be used to create high-performing, portable parts for the aviation and automotive sectors. Due to its unique properties, aluminum has long been used substantially in structural applications.It is excellent at resisting corrosion, robust but portable, & has superior thermal insulation. These metals are excellent because of their remarkable resistance to corrosion and low density, making them appropriate for usage in airplanes and automobiles[1]. Aluminum 8XXX alloys are widely employed in the plane industry from the start of the production of business aircraft. Duralumin, formerly referred to as Al-Cu-Mg alloy, became the initial alloy to be utilized in designing airplanesPrecipitation hardening serves as the main method of upgrading 8XXX aluminum alloys[2]. Copper is the primary ingredient within the 8xxx group of aluminum alloys, plus trace quantities of manganese and magnesium. This combination gives the alloy great machinability, substantial strength, and great shapeability. The

* Corresponding Author: arunsrinivas14@gmail.com

precipitation stiffening relationship among magnesium and copper is the origin of the sturdiness. These metals are renowned for having outstanding anti-corrosion properties in conditions that tend to be acidic and alkaline. They can be used in aeronautical definitionsalongside additional parts that require corrosion protection because of this property. The 2xxx series of alloys are suitable for applications requiring intricate shapes and precise tolerances due to their high formability. Additionally, heat treatment can be applied to them to improve their mechanical qualities. Because of this, as the alloys are perfect for use cases such as hydraulic components and aircraft themes[3-4].

Al-4.5%Cu alloy aluminum (AA8011) The metal, which has a 4.5% copper content, is widely used in both the aviation and automotive sectors due to the fact provides an outstanding strength-to-weight ratio and good machining ability. Because of its capacity to withstand extreme temperatures, it is a well-liked material for parts that must function in hot conditions, such motor and wing elements. Numerous studies have examined the effects of the alloying components on the dissolution behavior of alloys made of aluminum and how these changes impact the characteristics, functioning, and behavior of the materials below fatigue that is and creep constraints [5-6]. 7.Naik, R.B., Ratna, [7] 513°C was found to be the ideal solutionzing the environment in a research on the effects of extreme heat on the AA8011 alloy. A longer incubating period was associated with a buildup in severity whenever the temperature were under 503°C. Valli Gogula, Kuldeep K, [8] performed hot tensile experiments at six various temperatures, spanning from ambient temperature to 300°C, in order to investigate the mechanical characteristics of the AA8011 metal They discovered that sub-grain development during the molding process is responsible for the increased yield strength and ultimate tensile strength seen at lesser temperatures. 9. B Dharavath, MT Naik**, [9]** examined the mechanical properties of the steel alloys AA2014-T6 when it was exposed to tension along with compression loads in quasi-static & active settings.

The capacity of an alloy to be molded into a certain shape with no cracking or thinning down too much is known as sheet metal flexibility. But every piece of metal has a forming limit curve (FLC) that indicates how much further deformation it can withstand. Concentrated necking usually affects the FLC and can result in fractures that are ductile. The forming limit diagram (FLD) represents the major strains ($\varepsilon\varepsilon 1$) at the start of regional binding along with the minor strains ($\varepsilon\varepsilon 2$). This line graph represents the FLC. There are two distinct branches inside the FLC: the "left stem" & the "right stem." Positively major & minor strains are covered by the right sector, whereas positive major & negative minor strains are covered by the left stem.The FLC is derived from different main and minor strains ratios and is applicable only to proportionality strain routes. Figure 1 illustrates the forming limit diagram [10-11].

Ji He , Z. Cedric Xia [12] Plotting the experimental FLD, stretch formation of ASS 316 was carried out employing a hemisphere- punch throughout a temperature range of ambient (RT) to 400. A hypothetical forming limit diagram (FLD) suggested by the Marciniak-Kuczynski model is contrasted to a practical FLD that was made. The results of their study demonstrated that the FLD exhibited a preponderance of significant strain variations and that the ability to shape of the alloy was significantly influenced by the commencement of dynamic strain wrinkles.S. Qin, H.M. Shang,[13] discovered the 6061 aluminum alloy's cold forming restriction and came to the conclusion that In particular in the tension-tension area, the formation limit of the AA6061 tubing is almost twice that around the surrounding temperature at −196 °C. It plays a major role in the formation of intricate features below biaxial strain. 14.Sandeep Pandre,Ayush, [14] contrasted the results of many tests, including Swift Cu and Fukui's cylindrical Cup Drawings Test, to assess the flexibility of

steel & brass. Xugang Wang, [15] created a Nakazima check that is appropriate for assessing the flexibility of thinner copper strips. The results show that FLCs formed using the Nakazima test were comparable to those produced with the original Marciniak technique, leading to a low major strain level that is close to a plane strain condition.R. Karthik Rao et.al, [16] found that when temperature rises, radial expansions in tubes rises after examining the forming behavior of AA8011narrow tubes.

Lade Jayahari et.al, [17] used DYNAFORM program with LS-DYNA network to do finite element analysis on Ti-6Al-4V alloy at 400 °C for stretched forming. The results have been contrasted with actual data, and it was shown that Barlat 1989 output criteria forecast is more reliable than Hills 1948. Lumelskyj et.al, [18] used finite element analysis to produce FLCs for one complete circular sample with a radius of 55mm & six samples with different thicknesses (30, 50, 60, 77, and 99 mm). In the middle location where collapse was anticipated, samples were split into finite element grids with a dimension of the elements of h = 0.5 mm. For the simulations, the Nakazima check paradigm was used, with the assumption of an ongoing blow speed of 1 m/s. The researchers came to the conclusion that it was feasible to calculate FLCs utilizing finite element simulations by contrasting the numerical findings to the real-world FLC. Nejia Ayachi, [19] Utilizing the Nakazima Test Simulation Application, they created FLD for AA8011. They subsequently verified the simulation program by comparing the outcomes of the simulations with the actual experimental information. Given that the FLCs produced by software and testing techniques exhibit a substantial concordance, there is substantial agreement. L.Venugopal et.al, [20] After conducting an analysis, they discovered that the reusable strips of metal 2014-T6 had tiny structures made up of very extended grains that contained an extensive amount of second-phase atoms (with sizes that ranged from 5 to 10 μm) that were oriented in the path of operation. It was determined by SEM-EDS research revealed the particles involved were Al2Cu & Fe-Mn-Al. However, using a scanning electron microscope to study the frictional deposition in its original state, tiny, equivalent grains smaller than 3 μm in dimension were found. There didn't seem to be any grain roughening caused by warming actions since the size of the grain was uniform throughout each layer.

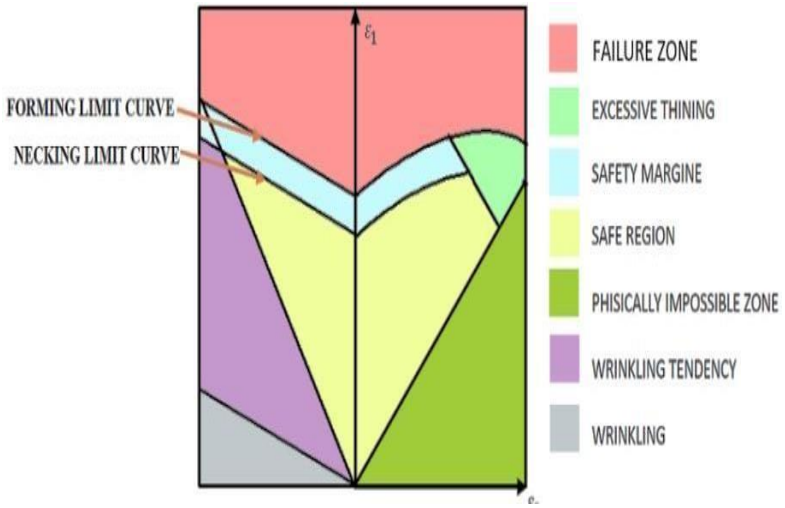

Fig. 1. FLD

The flexibility of layers and radial growth in pipes improve as the degree of heat gets higher in the present investigation, where FLD displayed at assessed temperatures (open

space temperatures, 100°C, 150°C) using an average strain of 0.01mm/s. In previous research, the flexibility of AA 8011 containers was performed out at an examined temperature along with the microscopic analysis was finished. A comparison is made between the fractography experiments carried out using a scanning electron microscopy and FLD produced by models and experiments.

2 Experimental details

2.1 Material specifications

A piece of AA 8011with a thickness of 1.0 mm was used as the substrate of interest in this investigation. After analysis, the molecular makeup of the AA 8011 metal sheets was noted in Table 1. This alloy, which has a copper content of 4.5%, is beneficial to the AA 2014 aluminum alloy since it makes the material stronger, harder, and more resistant to abrasion and rust. This enhances the alloy's capacity for conductivity to electricity as well as its resistance to elevated temperatures.

Table 1. Chemical composition of AA2014 sheet

Element	Composition (wt.%)
Al	92.86
Cu	4.415
Mg	0.568
Fe	0.136
Ti	0.0196
Zn	0.045
Mn	0.766
Si	0.898
Cr	0.0067
Other Elements	0.064

2.2 Nakazima Test (Hemispherical Dome test) for Stretch Forming

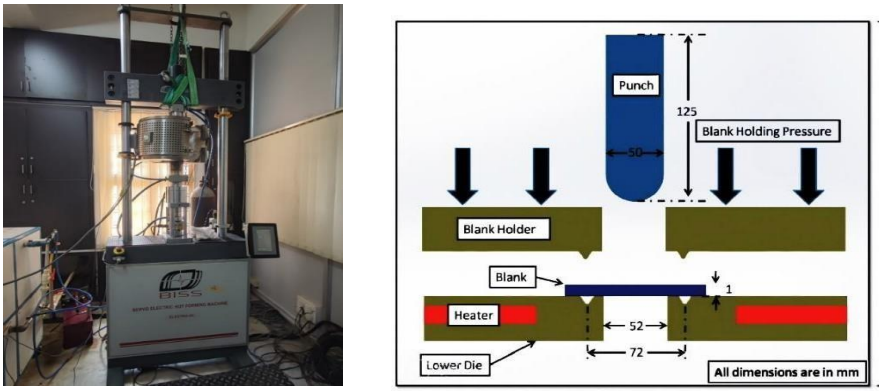

Fig.2. a) Experimental setup; b) Schematic Diagram

In the investigation, a 20-tons hydraulic presses was used to stretch AA2014 substance. The presses had a thermostat, a 2-zone splitting combustion chamber, and robotic regulation to preserve a steady temperature within ± 3% of the measured value. Its speed limit was 0.00001mm/min - 250mm/mi. The empty holding plates consisted of a notched beads to limit the entry of materials through the opening, and the extensible device contained a 50 millimeters diameter hemispherical dome-like punch. The second figure depicts the bending arrangement and the range of sample dimensions that were employed. After the deformation procedure, the task included cutting circle matrices on the prepared surfaces utilizing a dimension of 2.5 mm so that stresses could be measured with a traveling microscopy instrument. Three conditions of temperature were used for the task: the ambient temperature, 100°C, and 150°C. The punching speed used was 0.01 mm/s. In this investigation, the forming limit diagrams (FLD) was plotted using three distinct material kinds (see Figure 3(a)–(c)). b)

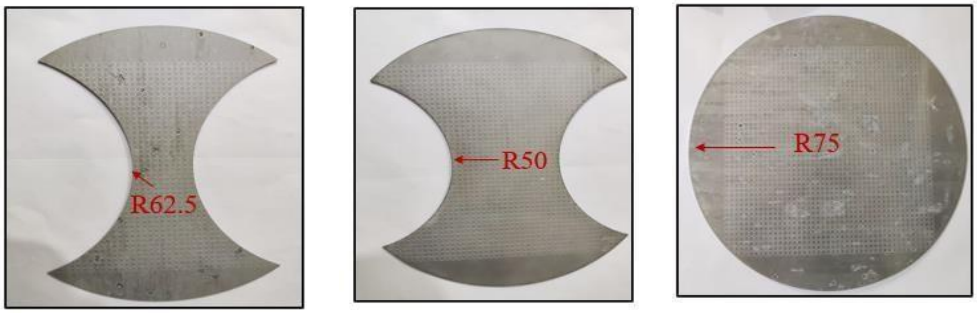

a) b) c)

Fig. 3. specimens for Nakazima test a) R62.5; b) R50; c) R75

3 Simulations

3.1 Mesh generation and 3D modelling

The method of evaluating with a finite element (FE) simulations entails modeling the tools required and connecting them effectively. Solid Works (SW) was used to generate the instrument and empty geometry in this research, while the files were kept in Steps formats. LS-Dyna was then used for importing those images. Starting and final boundaries, together with process variables, were specified after the meshing procedure was finished. Among the instruments, the blank piece was identified as the malleable body and another as the stiff body.

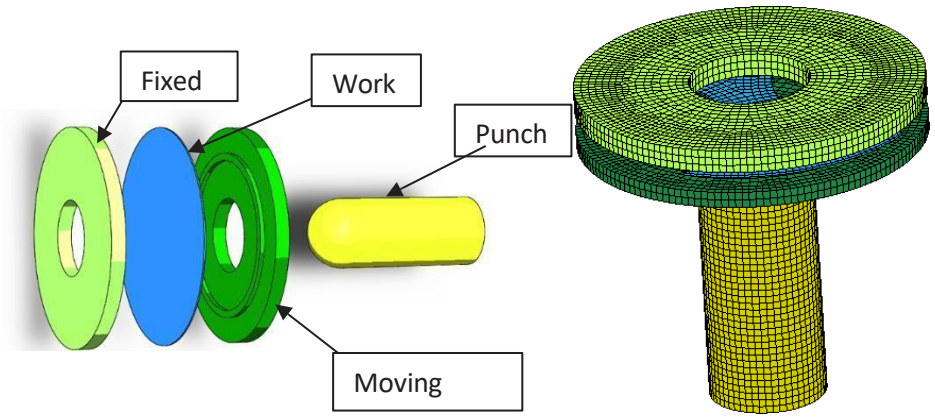

a) b)

Fig.4. a) 3D model for stretch forming; b) Finite element model.

3.2 FE Simulations

A method for modeling and researching how metals and buildings behave under various loading scenarios is called finite element analysis (FEA). In this method, the substance or building is divided to smaller, more manageable components known as finite components, and the mathematical problems governing the behavior of every component are solved. The behavior of the product or system as its entirety under different loading scenarios may therefore be predicted using the solutions for such calculations. When analyzing intricate structures or resources, like the alloy of aluminum 2014, where it is difficult to anticipate behavior using statistical techniques, FEA models are very helpful. Numerous physical processes, such as as distortion, tension, tension, and temperature behavior, may be modeled using these models. The entire effectiveness of an item or construction is predicted by summing the results of each constituent part. Tables 2 and 3 provide.

Table 2. Material properties taken for simulations.

YS (MPa)	Failure criteria	Elastic modulus (MPa)	r	N	Poisson's ratio (pr)	Mass density (kg/m^3)
463.802	0.18	7308	0.68	0.171	0.330	2795

Table 3. Process Parameters.

Diameter of hemispherical dome- shaped punch:	50mm
Blank material:	AA2014
Blank thickness:	1mm
Fixed and moved Plate Diameter:	150mm
Type of contact:	Forming one way surface to surface
Element type:	Rectangular and triangular
Blank element size:	3mm

The following is the choice of measurement elements:

- Components in the vicinity of the binding area are selected at arbitrarily.
- A regional binding state is confirmed by looking at the real stress worth, that is the material's Maximum Tensile Pressure number.
- In situations when binding was not seen, the modeling was carried out until a comparable stress level surpassed the genuine stress level related to the maximum tensile stress.

3 Results and discussions

3.1 Forming limit diagram (FLD)

Figure 5 shows the break history of many specimen types that popped at 0.01/s as well as at a variety of temperature . By use of a stereo microscopy, the samples' distortion throughout the Nakajima swelling phase was monitored. The progression of main and small strains may be estimated using the GOM-Correlate specialist software, and afterwards research can show different stages of distortion. The samples with different widths were found to undergo biaxial distortion initially, and then to move in a straight line. Its hemispherical punch's curve leads to departures from the optimal straight strain trajectories. Linear strains routes are typically derived in conjunction with Forming Limit Diagrams (FLD). The strike must make first contact against the specimen's centre in order to pass the Nakajima test. If the remainder of the non-contacting region does not undergo any deformation, the area that contacts zone will begin to bulge along the biaxial pressure strain route. The touching zone of the punch extends as it approaches into full engagement to the sample, resulting in the gradual development of a straight strain path that corresponds to its biaxial in nature pre-strain way.

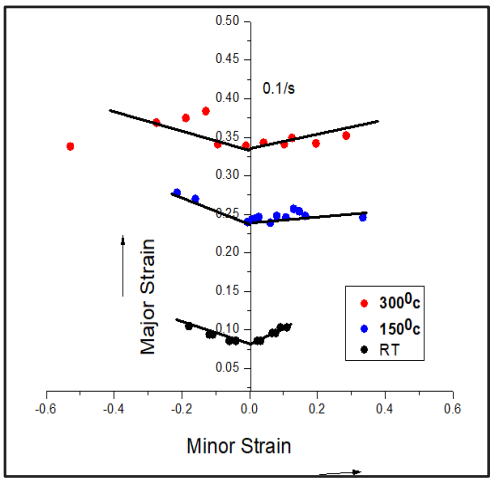

Fig. 5. FLD for different temperatures 300,150 and RT

During necking as a failing, or secure zone, the main and minor axis lengths are measured. A type of flaw known as necking develops whenever a metal sheets is too twisted in one spot, making it thinner and more compact elsewhereIt frequently happens during the metal's forming processes when the metal is subjected to high strains and rapid distortion. The necking effect can have serious consequences that affect the steel sheet's durability and

flexibility. A substance experiences a specific weakening once it shoulders, which may lead to cracking, tearing, or a complete explosion. This flaw may have a negative impact on the standard of the finished product and increase the likelihood of a component malfunctioning or failing.

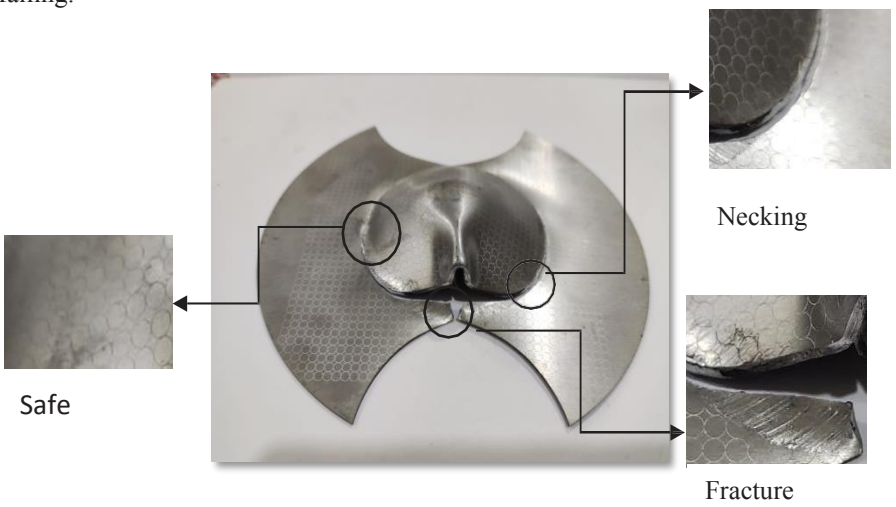

Fig.6. Necking, Failure, and Safe Regions of The Dome-Shaped Specimen

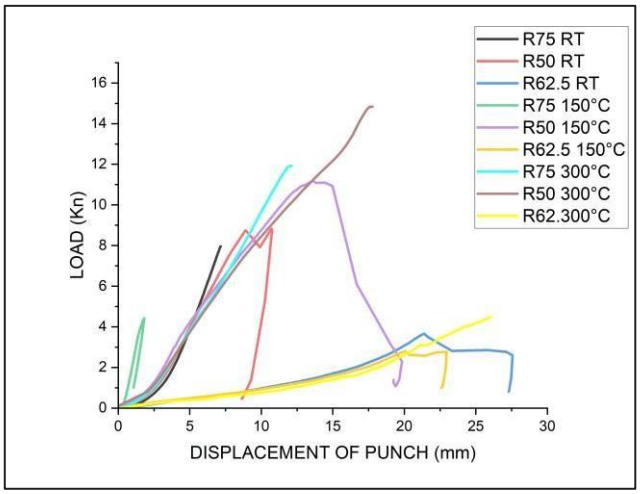

Fig. 7. Load vs Displacement graph

3.2 Limiting dome height.

restricting roof altitude (LDH) is an important parameter to know how easy it is to create multiple samples using various degrees. the level of LDH represents the specimen's altitude just before the break is about to occur. The mean LDH's dependent on temperature variation is shown in the figure. We saw that LDH was increasing as the experiment's temperature rose, which we attributed to this material thermal weakening. The flexibility, strain stiffening, thickness, and particle structure of the material are some of the characteristics

that affect LDH, which is an important aspect in metal sheeting.

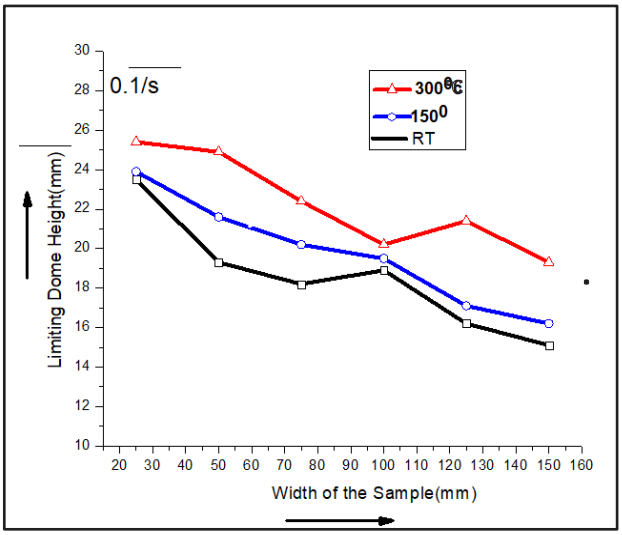

Fig. 8. variation of LDH

3.3 Analysis of AA8011

This study aims to establish the relationship between experimentally established limit strains that are anticipated by numerical models. Three distinct specimen were simulated and treated to different stress states at 150°C. The simulations produced distinct spots on the formation limit diagrams (FLD). Figure 10 shows the distorted geometry of all three samples at 150°C, while Table 4 presents the primary and secondary strains derived from models and tests. Every element's small and significant stresses were noted using the previously laid out selection standards.

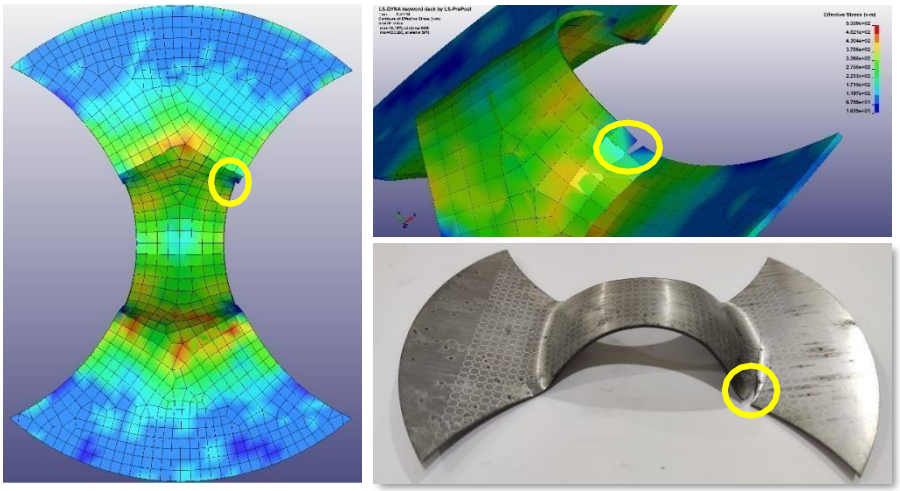

Fig. 9. comparison between the experimental sample and simulation result.

LS Dyna finite element program was used for simulating the Nakazima testing for AA 2014

evidence, and the measurement parts were selected in accordance with earlier discussions. To calculate the FLC of AA 8011, the components' main and small strains were obtained and displayed on a Forming Limit Curve (FLD) diagram.

Table 4. Experimental and FEM results

Specimen Dimensions (mm)	Experimental results		Simulation Results	
	Major Strain	Minor Strain	Major strain	Minor Strain
R75	0.24	0.31	0.28	0.33
R62.5	0.21	-0.18	0.23	-0.21
R50	0.16	-0.01	0.14	-0.03

Significant results are obtained from the studies, as evidenced by the high level of conformance and minor inconsistencies between the software-generated and practical FLCs.

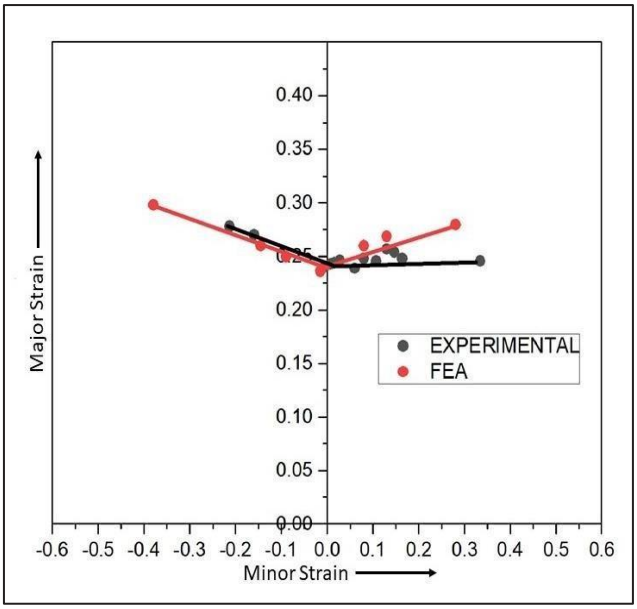

Fig. 10. FLD generated by experiment and FEA.

The findings of the simulation are employed to determine the stress caused by von Mises efficient plasticity and the resulting distortion. The greatest amount of stress level an object can withstand before undergoing deformation due to plasticity is known as the from Mises stress, also known as comparable or distorted potential stress. The calculation of the stress determined by von Mises depends on the multidimensional stress vector and takes into account the ordinary and shear loads operating on a substance. When anticipating breakdowns in materials and building structures that can resist expected loads, the stress assessment is a useful tool.

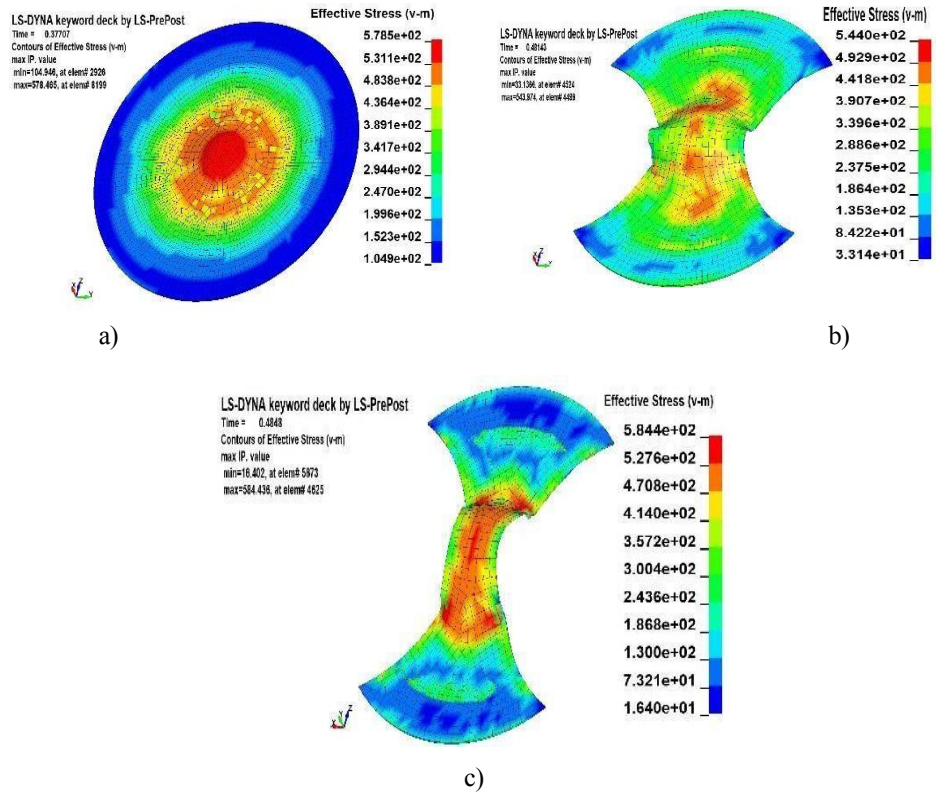

Fig. 11. Simulations result of a) R75; b) R50; c) R62.5.

Figure 11 illustrates the calculations that showed the 62.5 geometry to have the maximum stress effectively. The most effective stress is experienced by the location wherever the strike makes contact with the sample, whereas the non-forming zone suffers the lowest stress levels. Up to the breaking particular, the true stress rises as distortion develops.

measure of the deformation caused by plasticity a material experiences under mechanical force is called functional strain of plastic. Efficient plastic stress only evaluates the amount of plastic deformation in areas where the product has given past its elastic range, as contrast to total mechanical strain, which takes into account every plastic deformation that takes place within the substance. This characteristic is essential for figuring out how the material will behave under stress since it may be used to predict things such fatigue, breakdown of the material, and general resilience. In order to gain an understanding of how materials react with stress and create more durable constructions and products, researchers and developers employ a variety of testing techniques, including as tension and compressive tests, to measure effective stretch in plastic. A successful plastic stress is the long-term deformation brought on by pushing a material over its elastic limits.

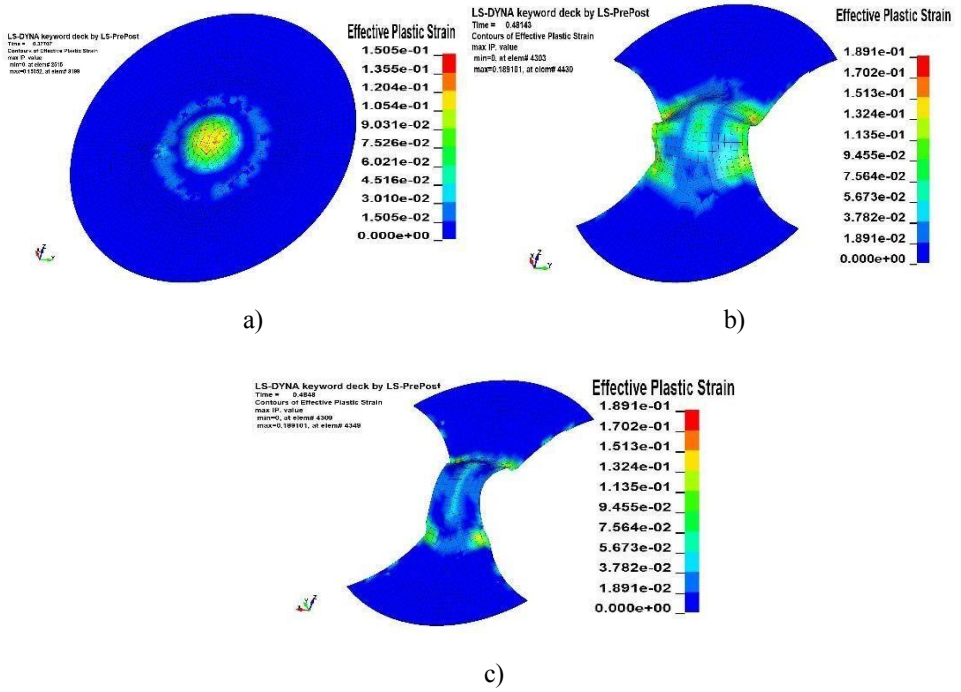

Fig. 12. Simulations result of a) R75; b) R50; c) R62.5.

The greatest EPS value between R62.5 and R75 occurred near the center of the geometry, while the R50 geometric produced the greatest efficient plastic stress (EPS), according to the simulation outcomes displayed in figure 12. The maximin EPS associated with the R50 form was discovered near the dome's margins. It was also observed that a rise in displacement was accompanied with a spike in EPS.

In the study of finite elements, the overall movement of an object or component as an outcome of the forces exerted or a specific amount of time is referred to being the consequent displaced. It is calculated by working through a series of formulas that represent how the structure will behave under specific loading conditions. The resulting displacement's amount as well as direction may be ascertained and utilized to assess the structure's general distortion and safety. In design for engineering, precise calculation of the resulting displacement is essential to guarantee that the building can bear required pressures and last throughout its lifespan. These calculations are usually carried out using finite element analysis programs, which may offer comprehensive details on the behavior of complex structures below different stress situations.

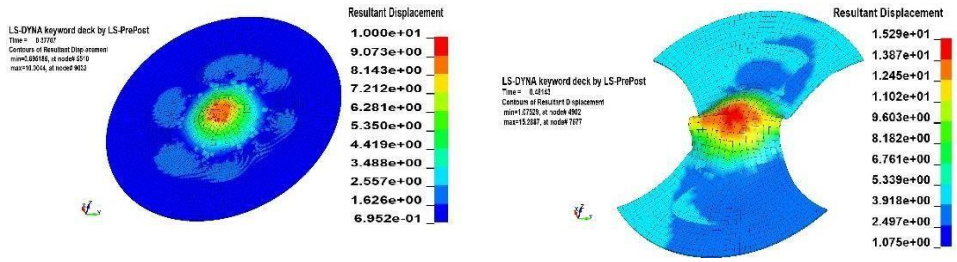

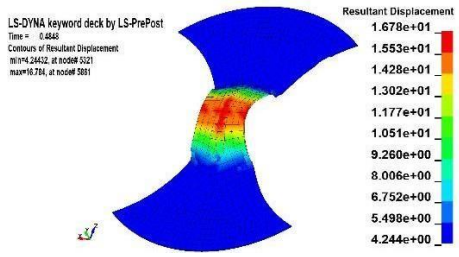

c)

Fig. 13. Simulations result of resultant displacement a) R75; b) R50; c) R62.5.

As can be seen in illustration 12, the value of R63.5 sample has a larger blow relocation, measuring 18.39 mm. This is due to the way it is shaped; as the punching movement grows, the tension rises. Punch dislocation values are similar in modeling and findings from experiments.

3.4 Microstructure Analysis

In fractography research, microscopy with scanning electrons (SEM) is a potent instrument that permits in-depth surface examination of broken materials. The investigation of a substance's surfaces that break to identify the root reason for failing is known as fractureography. With alloying components dispersed uniformly everywhere, a substance has a very fine, homogeneous structure. On the other hand, the alloy displays a more complex nanoscale structure made up of many phases. The α-Al lattice is the main component that gives the metal its durability and toughness .

4 Conclusion

- employing both experiments and FE modeling, the present study on AA8011 seeks to determine the forming limits at different temperatures. A summary of the research's main conclusions is provided follows.
- Utilizing the Nakajima test procedure, the forming behavior of the AA8011 alloy had been examined from the ambient temperature to 300°C at intervals of 150°C.
- For AA8011, the Forming Limit Diagram (FLD) was developed and scientifically calculated at the ambient temperature, 100°C, and 150°C.
- The minimal error among the FLD produced by the LS Dyna simulations tools and the actual experimental FLD at 150°C was noted.
- It was noted that drawing AA8011 metal to 150°C is challenging, while the temperature at which it was tested rose, LDH was seen to be increasing.
- In the dome-like cups, failure & binding were seen.
- Microstructure evaluation proved evident that all of the research's instances had brittle fractures.

References

1. Nitin Kotkunde, Amit Kumar Gupta, Prudvi Reddy Paresi, Swadesh Kumar Singh, Materials Today: Proceedings Volume 4, Issue 4, 2017.
2. Jayahari Lade ,Dharavath Baloji ,M.Sai sharath ,G.Raju1 ,Anil Kalluri ,A.Anitha Lakshmi , Minakshi Memoria “Finite Element Analysis on Experimental Stretch

Forming Process of AA2014 Alloy at 423 to 623K Temperatures", E3S Web of Conferences , 011 (2023) ICMPC 2023
3. Jürgen HIRSCH, Transactions of Non ferrous Metals Society of China, Volume 24, Issue 7, (July 2014).
4. TolgaDursun, Costas Soutis, Materials & Design (1980-2015) Volume 56, (April 2014),
5. R. Baloji Naik, D. Ratna, S.K. Singh." Synthesis and characterization of novel hyperbranched alkyd and isocyanate trimer based high solid polyurethane coatings" Progress in Organic Coatings Volume 77, Issue 2, February 2014, Pages 369-379
6. .S. P. Ringer, T. Sakurap And I. J. Polmear, Acta Materialia, Volume 45, Issue 9, September 1997
7. Naik, R.B., Ratna, D., Singh, S.K., Synthesis and characterization of novel hyperbranched alkyd and isocyanate trimer based high solid polyurethane coatings, Progress in Organic Coatings, 2014, 77(2), pp. 369–379
8. Tanya Buddi, Susmitha Valli Gogula, Kuldeep K. Saxena, Manufacturing and Evaluation of Mechanical Properties for Rice Husk Particle Board Using IoT , Indian Journal of Engineering & Materials Sciences: Volume 29, Issue 6, December 2022
9. B Dharavath, MT Naik, A Badrish, T Buddi, Experimental and Finite Element Studies of Stretch Forming Process for ASS 316L at Elevated Temperature, Indian Journal 2022 - ischolar.sscldl.in Volume 29, Issue 6, December 2022
10. B. Taleb Araghi, G.L. Manco, M. Bambach, G. Hirt" Investigation into a new hybrid forming process: Incremental sheet forming combined with stretch forming" CIRP Annals Volume 58, Issue 1, 2009, Pages 225-228K.
11. Woei-Shyan Lee, Chi-Feng Lin" Plastic deformation and fracture behaviour of Ti–6Al–4V alloy loaded with high strain rate under various temperatures" Plastic deformation and fracture behaviour of Ti–6Al–4V alloy loaded with high strain rate under various temperatures
12. Ji He , Z. Cedric Xia , Xinhai Zhu , Danielle Zeng , Shuhui Li , Sheet metal forming limits under stretch-bending with anisotropic hardening, International Journal of Mechanical Sciences Volume 75, October 2013, Pages 244-256
13. S. Qin, H.M. Shang, C.J. Tay, J. Mo "Stretching during axisymmetrical forming of sheet metal"Journal of Materials Processing Technology Volume 63, Issues 1–3, January1997,Pages117-122
14. Sandeep Pandre,Ayush Morchhale,Nitin Kotkunde &Swadesh Kumar Singh" Influence of processing temperature on formability of thin-rolled DP590 steel sheet"Pages 901-909 | Received 03 Feb 2020, Accepted 09 Mar 2020, Published online: 21 Apr 2020
15. Xugang Wang, Xiaobo Fan, Xianshuo Chen, Shijian Yuan, Journal of Materials Processing Technology Volume 306, August 2022
16. R. Karthik Rao , Phaneendra Babu Bobba , T. Suresh Kumar , Satyanarayana Kosaraju, Feasibility analysis of different conducting and insulation materials used in laminated busbars. Materials Today: Proceedings, 2019, 26, pp. 3085–3089
17. Lade Jayahari, P.V. Sasidhar, P. Prudvi Reddy, B. BaluNaik, A.K. Gupta,Swadesh Kumar Singh, Formability studies of ASS 304 and evaluation of friction for Al in deep drawing setup at elevated temperatures using LS-DYNA, Journal of King Saud University - Engineering Sciences, Volume 26, Issue 1, 2014, Pages 21–31.
18. J. Pavan Kumar, R. Uday Kumar, B. Ramakrishna, B. Ramu and K. Baba Saheb 2nd International Conference on Advancements in Aeromechanical Materials for Manufacturing, volume 455, July 2018.
19. Nejia Ayachi, Noamen Guermazi, Cong Hanh Pham. Metals 2020, 10(9), 116, August 2020.

20. L. Venugopal, M. J. Davidson & Material and manufacturing process, volume 28, issue 3, 2013
21. Suresh Kumar Tummala, Phaneendra Babu Bobba & Kosaraju Satyanarayana (2022) SEM & EDAX analysis of super capacitor, Advances in Materials and Processing Technologies, 8:sup4, 2398–2409.
22. Lumelskyja, J. Rojeka, L. Lazarescub, D. Banabic, Procedia Manufacturing, Volume 27, 2019
23. B. J. Varghese, P. B. Bobba and M. Kavitha, "Effects of coil misalignment in a four coil implantable wireless power transfer system," 2016 IEEE 7th Power India International Conference (PIICON), Bikaner, India, 2016, pp. 1–6
24. Mahalle G, Morchhale A, Kotkunde N, Gupta AK, Singh SK, & Lin Y C, J Manuf Processes, (2020) 482.
25. L. Venugopal, M. J. Davidson & N. SelvarajMaterial and manufacturing process, volume 28, issue 3,2013.